Energy and Z_2 dependences of energy straggling for fast proton beams passing through solids

Yoshiaki Kido
Toyota Central Research and Development Laboratories, Inc., 41-1, Aza Yokomichi, Oaza Nagakute, Nagakute-cho, Aichi-gun, Aichi-ken, 480-11, Japan
(Received 17 December 1985)

The energy and Z_2 (target atomic number) dependences of energy straggling for fast proton beams are investigated using nuclear resonance reactions of $^{19}F(p,\alpha\gamma)^{16}O$ and $^{27}Al(p,\gamma)^{28}Si$. The results are compared with theoretical predictions based on the free-electron models (of Bohr and of Vavilov) and the local-electron-density models (of Lindhard and Scharff and of Chu). Concerning both energy and Z_2 dependences, the experimental data agree well with Chu's prediction using the Hartree-Fock-Slater charge distributions of the target atoms.

I. INTRODUCTION

A fast ion that penetrates a medium loses its energy via a number of successive collisions. This leads to statistical fluctuations in the energy loss of the ion beam around its average value, i.e., energy straggling. The values of the energy straggling for light ions are important parameters for simulation of a Rutherford backscattering spectrum and an excitation spectrum for a nuclear resonance reaction in ion-beam analysis.[1,2]

In the high-energy region above several tens of keV/amu, electronic interactions dominate the slowing-down process of a fast ion beam. So far, two different theoretical approaches have been developed concerning electronic straggling. One derives an accurate energy distribution function by solving a transport equation. This approach originated from Landau's formalism[3] and was then extended by Vavilov[4] under the assumption that all the target electrons are free. Another calculates directly the full width at half maximum (FWHM) of the energy-loss distribution assuming it to be a Gaussian. In the high-energy limit where all the target electrons are considered free, Bohr[5] derived the simple expression given by

$$\Gamma_B^2=(32\ \ln 2)\pi Z_1^2 Z_2 e^4 N\Delta R\ , \tag{1}$$

where e is the electron charge, Z_1 and Z_2, the atomic numbers of the projectile and the target atoms, respectively, and $N\Delta R$ the target thickness (atoms/cm^2). Lindhard and Scharff[6] extended Bohr's treatment by considering the local electron density of the target atom. The reduced straggling is expressed by

$$\Gamma^2/\Gamma_B^2=\frac{1}{Z_2}\int_0^\infty 4\pi r^2\rho(r)\frac{\Gamma^2(\rho(r),v)}{\Gamma_B^2}dr\ , \tag{2}$$

where $\rho(r)$ denotes the electron density of the target atom, $\Gamma^2(\rho(r),v)$ the contribution from various parts of the electron cloud to the straggling. They proposed the simple asymptotic formula

$$\Gamma^2/\Gamma_B^2=\begin{cases}L(\chi)/2 & \text{for } \chi\lesssim 3\ ,\\ 1 & \text{for } \chi\gtrsim 3\ ,\end{cases} \tag{3}$$

where $L(\chi)=1.36\chi^{1/2}-0.016\chi^{3/2}$. Here, χ is a reduced energy variable defined by $\chi=v^2/(Z_2 v_0^2)$ (v is the ion velocity, and v_0 the Bohr velocity). Bonderup and Hvelplund[7] refined this model by using the electron charge density $\rho(r)$ calculated from the Lenz-Jensen model. Similar calculations based on the Hartree-Fock-Slater model were carried out by Chu.[8]

Up to now, several experimental results on electronic straggling have been reported.[9–14] However, there are large discrepancies not only between experimental data and theoretical predictions but also between different measurements. This is probably due to the target conditions such as texture and film nonuniformity, which yield additional contributions to the energy straggling. As experimental methods, the backscattering or transmission technique combined with solid-state detectors has been usually employed. In the transmission experiment, we must prepare self-supporting target foils smoothed out, and we frequently need backing foils to prevent their breakage. On the other hand, the backscattering spectrum includes the contributions from the incoming and outgoing paths in the target film. These situations cause inaccuracies in determining the straggling values. In addition, the energy resolution of solid-state detectors is only 10 keV at best. Thus, in order to get accurate straggling data, the transmission technique with a magnetic or electrostatic spectrometer is most desirable. So far, only a few reports on straggling measurements using this technique have been made for heavy ions (lithium, nitrogen, and neon) passing through solids[15,16] and for proton and helium in gases.[17]

In the present experiment, we employed a new technique using nuclear resonance reactions with narrow natural widths. The nuclear reactions of $^{19}F(p,\alpha\gamma)^{16}O$ and $^{27}Al(p,\gamma)^{28}Si$ were used for this purpose. This technique makes it easy to prepare a variety of thin and smooth target films and gives good energy resolution. The principle of this method is to derive the straggling width from the slope of the excitation spectrum of γ-ray yields for the Al or LiF substrate onto which a thin target film is deposited. In order to obtain accurate straggling values, the excitation spectrum is generated theoretically

and then fitted to the experimental one by varying the thickness of the target film and the straggling value of interest. Thus, energy and Z_2 dependences of the energy straggling are investigated for 20 elements as targets. Our concern is centered on checking the validity of the theoretical models proposed so far. Finally the reduced energy straggling is expressed as a function of beam energy explicitly.

II. EXPERIMENT

The experimental procedure is described in detail in the previous work.[18] The utilized nuclear reactions are $^{27}Al(p,\gamma)^{28}Si$ at 992 keV with a FWHM (Γ_r) of 0.1 keV and $^{19}F(p,\alpha\gamma)^{16}O$ at 340, 484, and 872 keV with FWHM's of 2.5, 0.9, and 4.5 keV, respectively. The nuclear reactions occur within the thick polycrystals of LiF or Al films deposited onto Si wafers.

Target films were evaporated onto mirror-finished LiF polycrystals or Al-evaporated Si wafers with an electron beam. The substrates were rotated around a hearth during evaporation so as to obtain homogeneous films. The thickness of the target film was measured by Rutherford backscattering using a 2.0-MeV $^4He^+$ beam. A thin Al film deposited onto a C-evaporated NaCl crystal was used as a film-thickness standard for the backscattering measurements. The thickness of this Al film was determined using the nuclear resonance reaction of $^{27}Al(p,\gamma)^{28}Si$ at 992 keV. As the stopping power value of Al for the 992-keV H^+ beam, we used the semiempirical formula given by Andersen and Ziegler.[19] The thicknesses of the target films range from 80 to 250 nm. Figure 1 shows the surface profiles of the Al films deposited onto a Si wafer and onto a LiF polycrystal. The degree of surface roughness is estimated to be 5 to 7 nm from a surface profile measurement. Its lateral resolution is better than 2 nm.

A well-collimated proton beam impinged on the target tilted to 45° with the incident-beam axis (Fig. 2). The emitted γ rays were counted with a 115-cm^3 Ge(Li) detector placed 3 cm apart form the target. The incident-beam energy was determined accurately from the deflection by the magnetic field which was measured with a proton magnetic resonance. The excitation spectrum of γ ray yields was obtained by varying the incident-beam energy in the vicinity of the resonance energy.

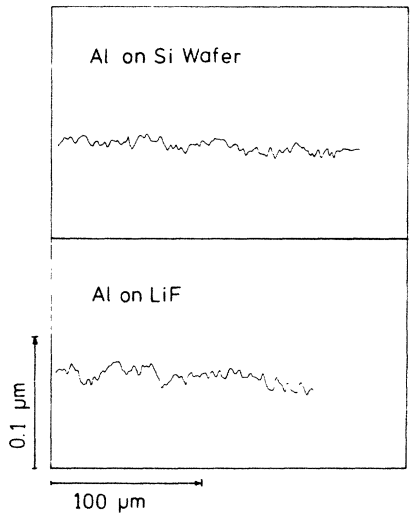

FIG. 1. Typical surface profiles of Al evaporated onto a Si wafer (upper) and onto a LiF polycrystal (lower). The lateral resolution of a profilometer is better than 2 nm.

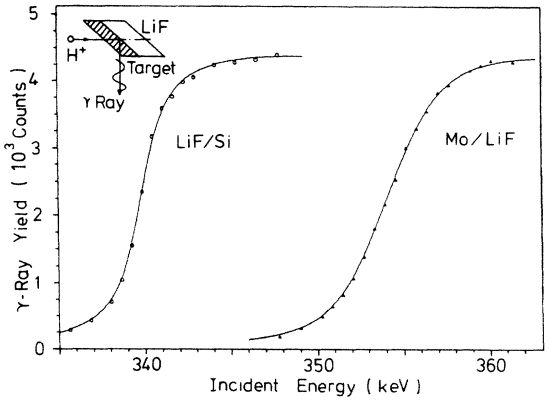

FIG. 2. Excitation spectra around the 340-keV resonance of $^{19}F(p,\alpha\gamma)^{16}O$ for LiF/Si and Mo/LiF targets. The solid curves correspond to the simulated spectra best fitted to the experimental data. The deviations from the experimental results are less than 0.4% for both the LiF/Si and Mo/LiF cases. The fitting parameters used are as follows: $\Gamma_0^2=0.20$ keV^2, $\Gamma_s^2=18.0$ keV^2, and the effective thickness of the Mo film, $t=4.90\times10^{17}$ atoms/cm^2.

III. DATA ANALYSIS

As a typical example, we treat the case of the 340-keV resonance of $^{19}F(p,\alpha\gamma)^{16}O$ for LiF/Si and Mo/LiF targets. The emitted γ-ray yields are plotted as a function of the incident-beam energy in Fig. 2. In order to determine the straggling values accurately, the excitation spectrum of the γ-ray yields is simulated and best-fitted to the experimental one. In the synthesis of the excitation spectrum, we subdivide the depth of the LiF film into many thin slabs with equal widths Δx. The contribution from the kth slab counted from the top surface is calculated from

$$\Delta Y_k(E_i)=\int_{E_r-10\Gamma_r}^{E_r+10\Gamma_r}\frac{cF(E_{ik}-E)}{(E_r-E)^2+\Gamma_r^2/4}dE\ , \tag{4}$$

$$E_{ik}=E_i-\Delta E_{ik}=E_i-k\Delta x\left[\frac{dE}{dx}\right]_{\mathrm{LiF}}\ , \tag{5}$$

where E_i and E_r are the incident-beam energy and the resonance energy (340 keV), respectively, c, the constant for normalization, and $(dE/dx)_{\mathrm{LiF}}$ the stopping power of LiF for protons. We assume a Gaussian energy-loss distribution expressed by

$$F(E_{ik}-E)=\frac{2\sqrt{\ln 2}}{\sqrt{\pi}\Gamma_{tk}}\exp\left[-\frac{4\ln 2}{\Gamma_{tk}^2}(E_{ik}-E)^2\right]\ , \tag{6}$$

$$\Gamma_{ik}^2=\Gamma_0^2+\Gamma_{sk}^2\ , \tag{7}$$

where Γ_0 and Γ_{sk} are the FWHM's of the initial energy spreading of the incident beam and the straggling value of the proton beam arriving at the kth slab, respectively. The total γ-ray yield from the LiF film is given by

$$Y(E_i)=\sum_k \Delta Y_k(E_i) . \tag{8}$$

For the LiF substrate onto which the target film is deposited, we must add the contributions of the energy loss and energy straggling in the target film for Eqs. (5) and (7). For the slowing-down process of fast protons in the target film, we used the semiempirical stopping powers tabulated by Andersen and Ziegler.[19] Bohr straggling values and additivity rules on the stopping power and energy straggling were assumed for the compound material of LiF. The availability of Bohr straggling values for LiF is assured by the following two reasons. First, Bohr values are used also for the LiF/Si target in determining the initial energy spreading of the incident beam. Therefore, the influence of the above assumption is almost canceled, as can be seen from Eq. (7). The second is, as shown in the next section, the fact that the experimental straggling values agree with Bohr's predictions for low-Z materials.

The initial energy spreading of the incident beam is determined by fitting the calculated excitation spectrum to the experimental one for the LiF/Si target. As shown in Fig. 2, the slope of the excitation curve for the Mo/LiF target becomes gentle compared with the LiF/Si case because of the energy straggling of the proton beam passing through the Mo film. The best-fitted excitation spectrum is obtained by adopting the appropriate values of the target thickness and the energy straggling of interest.

Now, we must check the validity of the assumption that the energy-loss distribution is a Gaussian. For very thick targets, the stopping cross sections cannot be considered independent of the beam energy and the energy-loss distribution deviates from a Gaussian. Tschalär[20] derived the critical condition for the target thickness that the average relative energy loss $\Delta E/E$ does not exceed about 20%. For a high-energy beam passing through a thin target film, Vavilov[4] showed that the energy-loss distribution becomes asymmetric with a high-energy tail. In Fig. 3, the energy-loss distribution derived from the present experiment is compared with the Vavilov's prediction for the 340-keV proton beam passing through a Mo film with thickness 4.53×10^{17} atoms/cm^2. As clearly seen, the Vavilov distribution can be regarded approximately as a Gaussian under this condition. In the present work, the target films with thickness 80 to 250 nm were prepared so that the energy-loss ratio ranged from 3 to 6% and the assumption of a Gaussian energy distribution is valid.

Before showing the experimental results, we discuss the additional contributions of the energy straggling from the effects of texture (small crystallites forming the film), nonuniform film thickness, the spatial correlation, and projectile charge-state fluctuations. The texture effect is neglected in this experiment, because no channeling effect was observed in the backscattering spectra for the present target films. Furthermore, it was confirmed by reflection electron diffraction that there exist no significant crystal-

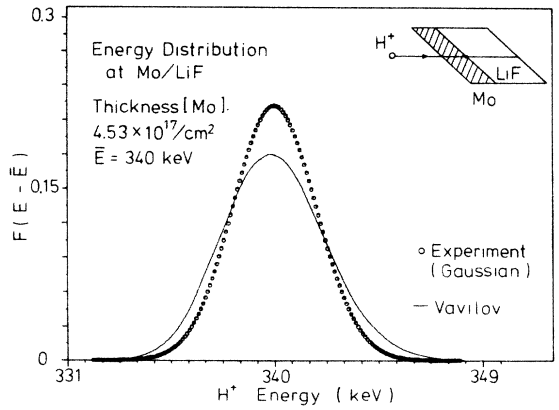

FIG. 3. Energy distributions of a proton beam with average energy 340 keV just arriving at the interface between Mo and LiF. The effective Mo thickness is 4.53×10^{17} atoms/cm^2. The plotted spectrum corresponds to the experimental result obtained assuming a Gaussian shape while the distribution calculated from the Vavilov theory is depicted by the solid curve.

lites in the target film. In order to estimate the contribution from film nonuniformity, we use the following relation:

$$\Gamma_i^2=8\ \ln 2(dE/dx)^2\delta x^2 , \tag{9}$$

where dE/dx is the stopping power of the target film and δx the standard deviation of the fluctuation of the target thickness. From the result of the surface profile measurement, we use the values of 5 to 7 nm for δx. As Besenbacher *et al.*[12] pointed out, the spatial correlation effect in the solid target is much smaller than in a gas target. Therefore, this effect is neglected in the present work. Concerning the charge-state fluctuation, Brandt and Sizmann[21] showed that the electron cannot be bound to the fast proton penetrating a solid medium due to collision broadening and collective screening by the valence electrons. It is natural to expect that neutral hydrogen atoms are formed at the exit surface. From the above discussion, the total energy straggling observed is approximated by

$$\Gamma_t^2=\Gamma_0^2+\Gamma_i^2+\Gamma_s^2 , \tag{10}$$

where Γ_s denotes the electronic straggling of interest.

IV. RESULTS AND DISCUSSION

Figures 4(a) and 4(b) show the energy dependence of the reduced straggling Γ/Γ_B for the proton beams passing through Al and Ni films, respectively. The solid circles and the experimental data corresponding to $[\Gamma_i^2+\Gamma_s^2]^{1/2}/\Gamma_B$ and the open circles, the corrected values Γ_s/Γ_B. The dotted and solid curves denote the theoretical values given by Lindhard and Scharff[6] and by Chu,[8] respectively. Vavilov's values coincide with Bohr's values within 1%. The experimental results support the local-electron-density models (of Lindhard and Scharff and of Chu) for both Al and Ni targets. There are large discrepancies between the experimental data and the

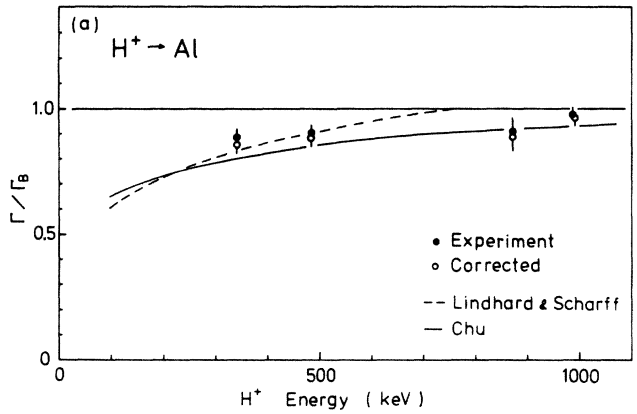

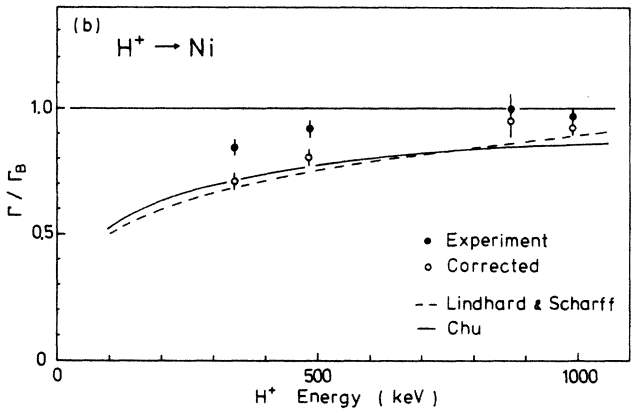

FIG. 4. (a) Reduced straggling values for the Al film plotted as a function of the incident energy of proton beams. The solid circles denote the raw data of the present experiment and the open circles, the data corrected for film nonuniformity. The solid and dashed curves are the theoretical predictions of Chu and of Lindhard and Scharff, respectively. (b) Reduced straggling values for the Ni film plotted as a function of the incident proton energy. The notation is the same as that used in (a).

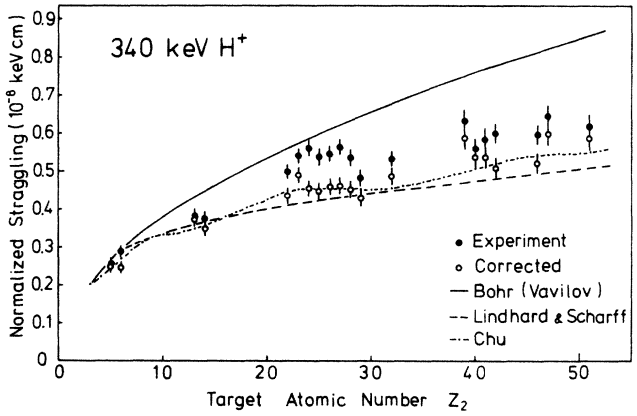

FIG. 5. Z_2 dependence of the normalized energy straggling for 340-keV proton beams. The solid circles are the raw data measured by the present experiment and the open circles, the data corrected for film nonuniformity. The solid, dashed, and dot-and-dash curves are the theoretical predictions given by Bohr, by Lindhard and Scharff, and by Chu, respectively.

theoretical values based on the free-electron models (of Bohr and of Vavilov) at the relatively low energies of 340 and 484 keV. Friedland and Kotze[13] reported the energy dependence of the reduced straggling for proton and deuteron beams passing through Cu foils. Their data are consistent qualitatively with the theoretical values calculated from the local-electron-density models, but 20–30% larger than Chu's values. We can expect that their results agree with Chu's prediction, if correction for the influence of foil inhomogeneity is made. Similar results were reported on the energy straggling of ^{4}He beams in Al, Ni, and Au foils by Harris and Nicolet.[9] Also in this case, one can expect the agreement between their data and Chu's values, if one subtracts the contributions from the effects of foil inhomogeneity and charge-state fluctuation. Besenbacher *et al.*[17] measured straggling values for hydrogen and helium ions passing through various gases in the energy range 40 to 1000 keV/amu. Their results for proton beams in Ne, Ar, Kr, and Xe are in good agreement with the sum of Chu's values and the spatial correlation term. The results presented above support Chu's model and, in addition, suggest the significant contributions from film nonuniformity for solid targets and from the spatial correlation of the atomic electrons for gaseous targets.

We can express approximately the energy dependence of the reduced straggling calculated from Chu's theory by

$$\Gamma/\Gamma_B = 1 - a\exp(-bE)/\sqrt{E} \ . \tag{11}$$

The coefficients $a=0.152$ and $b=0.8$ for Al and $a=0.181$ and $b=0.25$ for Ni targets. Formula (6) is very useful in simulating backscattering and excitation spectra.

Figure 5 shows Z_2 dependence of the normalized straggling for the 340-keV proton beams. The solid circles are the experimental data corresponding to $[(\Gamma_i^2+\Gamma_s^2)/N\Delta R]^{1/2}$ and the open circles, the corrected ones for $\Gamma_s/\sqrt{N\Delta R}$. Theoretical values given by Bohr, by Lindhard and Scharff, and by Chu are depicted by solid, dashed, and dot-and-dash curves, respectively. Vavilov's values are almost the same as Bohr's values. It is clearly seen that the corrected values agree with Chu's prediction within 5% except for the case of Y targets. Lindhard and Scharff's model gives too small straggling values for the target materials with relatively high Z numbers. For the Ag targets, the present datum agrees with the experimental one $[(0.625\pm0.027)\times10^{-8}$ keV cm] reported by Möller and Nocken[11] within experimental uncertainty. The experimental error in this work is estimated to be at most 5%. This originates mainly from film nonuniformity and the best-fitting process of the excitation spectrum.

V. CONCLUSION

The energy and Z_2 dependences of the energy straggling have been investigated systematically. The present

results certify the validity of Chu's prediction based on the Hartree-Fock-Slater model and reveal the significant contribution from the film nonuniformity for solid targets. The reduced straggling values calculated from Chu's model can be expressed approximately in a simple form as a function of a beam energy. This formula could be utilized for simulation of backscattering and excitation spectra with good accuracies. Concerning the Z_2 dependence of the energy straggling, this work may be the first attempt to get reliable and systematic data for proton beams with relatively low energies. The present results reveal that the atomic shell structures must be taken into account even in the fluctuation of the energy-loss distribution as a second-order phenomenon of the slowing-down process.

ACKNOWLEDGMENTS

I would like to acknowledge Dr. J. Kawamoto, Dr. T. Hioki, Dr. S. Noda, and Dr. H. Doi for valuable discussion on this work. Special thanks are also due to my colleagues, K. Yamada, M. Kakeno, A. Itoh, M. Ohkubo, and I. Konomi for their technical support of the experiment.

[1]P. A. Saunders and J. F. Ziegler, Nucl. Instrum. Methods **218**, 67 (1983).
[2]Y. Kido and Y. Oso, Nucl. Instrum. Methods **B9**, 291 (1985).
[3]L. Landau, J. Phys. USSR **8**, 201 (1944).
[4]P. V. Vavilov, Zh. Eksp. Teor. Fiz. **32**, 320 (1957) [Sov. Phys.—JETP **5**, 749 (1957)].
[5]N. Bohr, Philos. Mag. **30**, 581 (1915).
[6]J. Lindhard and M. Scharff, K. Dan. Vidensk. Selsk. Mat. Fys. Medd. **28**, No. 8 (1954).
[7]E. Bonderup and P. Hvelplund, Phys. Rev. A **4**, 562 (1971).
[8]W. K. Chu, Phys. Rev. A **13**, 2057 (1976).
[9]J. M. Harris and M-A. Nicolet, Phys. Rev. B **11**, 1013 (1975).
[10]G. E. Hoffman and D. Powers, Phys. Rev. A **13**, 2042 (1976).
[11]W. Möller and U. Nocken, Nucl. Instrum. Methods **149**, 177 (1978).
[12]F. Besenbacher, J. U. Andersen, and E. Bonderup, Nucl. Instrum. Methods **168**, 1 (1980).
[13]E. Friedland and C. P. Kotze, Nucl. Instrum. Methods **191**, 490 (1981).
[14]J. B. Malherbe and H. W. Alberts, Nucl. Instrum. Methods **192**, 559 (1982).
[15]H. H. Andersen, F. Besenbacher, and P. Goddiksen, Nucl. Instrum. Methods **168**, 75 (1980).
[16]P. Mertens, Thin Solid Films **60**, 313 (1979).
[17]F. Besenbacher, H. H. Andersen, P. Hvelplund, and H. Knudsen, K. Dan. Vidensk. Selsk. Mat. Fys. Medd. **40**, No. 9 (1981).
[18]Y. Kido and T. Hioki, Phys. Rev. B **27**, 2667 (1983).
[19]H. H. Andersen and J. F. Ziegler, *Hydrogen Stopping Powers and Ranges in All Elements* (Pergamon, Oxford, 1977).
[20]C. Tschalär, Nucl. Instrum. Methods **64**, 237 (1968).
[21]W. Brandt and R. Sizmann, Phys. Lett. **37A**, 115 (1971).